

Microstructure Evolution and Tensile Properties of 304L Stainless Steel Subjected to Surface Mechanical Attrition Treatment

Ping Jiang^{1*,a}, Jian Lu^{2,b} and XiaoLei Wu^{3,c}

^{1,3} State Key Laboratory of Nonlinear Mechanics, Institute of Mechanics, Chinese Academy of Science, Beijing 100190, People's Republic of China

² Department of Mechanical Engineering, The Hong Kong Polytechnic University, Hung Kom, Kowloon Hong Kong, People's Republic of China

^ajping@imech.ac.cn

^bmmlu@inet.polyu.edu.hk

^cxlwu@imech.ac.cn

Keywords: Surface mechanical attrition treatment; 304L stainless steel; gradient nanostructured layer; mechanical twinning; mechanical properties.

Abstract. A gradient nanostructured layer (GNsL) was generated on the two sides of bulk sample in 304L stainless steel by means of the surface mechanical attrition treatment. The microstructure of the GNsL was characterized via TEM observation. The prominent microstructural features involve the intersection of multi-system twin operation, subdividing the original grains into blocks, a martensite transformation mainly occurring at the interface of the twins as well, and the randomly orientated nanocrystallites at the top of surface. After annealing at 750°C for 10 min, recovery had occurred and the dislocation density was much reduced. The vast majority of the grains at the top surface were in the nanocrystalline/ultrafine range, with some recrystallization regions. The uniaxial tensile tests were performed to obtain the mechanical property of bulk samples with GNsL. The yield strength was about 2 times higher than that of the coarse-grained counterpart, but with a decrease in uniform elongation and elongation to failure as well. The relationship between the microstructure and mechanical property was discussed in detail.

Introduction

304L stainless steel (SS) is a widely used material for engineering and research. In recent several years, the investigations on microstructural evolution and mechanical properties by K. Lu, J. Lu and C.H. Huang have been carried out [1,2]. Because of the low stacking fault energy (SFE), mechanical twinning and dislocation slip dominate the deformation process through the application of severe plastic deformation, typically surface mechanical attrition treatment (SMAT) [1], equal channel angular pressing (ECAP) [2] and laser shock process (LSP) [3].

SMAT has recently been developed to produce a gradient nanostructured layer (GNsL) on the surface layer of bulk materials [4-6]. The process is based on surface dynamic plastic deformation induced by repeated impacts with high-velocity walls. The formation mechanism of the nanocrystalline (nc) surface during SMAT process has been investigated for different crystal structure and SFE metals. Typical mechanism for grain refinement mainly involves dislocation slip for high SFE materials [7,8], such as Fe and Al alloy, and mechanical twinning for low SFE materials [1,9], such as Ti and stainless steel. Many researchers have focused on the mechanical properties of SMAT samples including the nc-316L SS with about 15 μm thickness cut from the bulk SMAT sample [10], the surface nanocrystallised 316L SS bulk samples [11] and SMAT-nc-Cu with 14 μm thickness [12], and so on.

Based on the above investigations, the aim of the present work is to study the microstructure evolution and the mechanical properties after different SMAT process time and subsequent annealing. The relationship between the microstructure and mechanical property will be discussed in detail

Experimental

A cold-rolled 304L austenitic SS (Fe-0.02%C-18.92%Cr-8.06%Ni-1.07%Mn-0.39%Si) was used in the present investigation. The cold-rolled sheet with an average thickness of 1mm was annealed at 900°C for 4 h under vacuum. Sheets with a diameter of 100 mm were provided for the SMAT process. The detailed procedures of the SMAT process have been published in the previous literature [4]. In the present study, the SMAT was performed at room temperature for 30 min with a vibrating frequency of 20 kHz. To investigate the effect of post-process annealing on the microstructure and mechanical properties, the SMAT samples were annealed at 650 °C and 750°C respectively for 10 min under vacuum.

The transmission electron microscope (TEM, operating at 200 kV) and the corresponding selected area electron diffraction (SAED) were used to observe the microstructure evolution of different layers by polishing the corresponding layer until the thickness was about 30 μm , and followed by twin-jet polishing using a solution of 7% perchloric acid in alcohol at -30°C.

Tensile specimens with a gauge dimension of 14 mm \times 2.5 mm \times 1mm were cut from the SMAT sample. Tensile tests were performed on a MTS 810 test machine with displacement control and an extensometer. After installation of the extensometer the samples were deformed at an initial strain rate of 0.5 mm/min, corresponding to $5 \times 10^{-4} \text{ s}^{-1}$.

Results and Discussion

Microstructural Characterisation of the SMAT sample. For the 304L SS with a low SFE (about 16.4 mJ m⁻²), deformation twins and the martensite transformation play an important role in the grain refinement during SMAT process. Fig. 1a shows a TEM image of the microstructure of the SMAT 30 min 304L sample at about 30 μm deep, showing the twin lamellar structures, typically about 150nm width. Dense dislocation walls and dislocation pile-up are observed inside twins and matrixes visibly. Fig. 1b is a typical TEM images of low SFE metal microstructure subjected to a surface severe plastic deformation. Intersection of multi-system deformation twins in several directions results in submicro-sized blocks, a martensite transformation mainly occurring at the interface of the twins as well. As indicated by the white lines, multi-system deformation twins are visible and the intersectional angle between the twins aligned in different directions is about 70.5°. In addition, α' martensite phase (indicated by blue arrows) is also observed in the Fig. 1b and c. It is known that α' martensite transformation usually happens at the intersection of two sets of deformation twins [13,14]. The dislocations with high density near the top surface, together with plenty of intersections of twins make the martensitic nucleation easier at high strain and strain rates. It can be clearly seen that the grain size of the α' phase is about 100-200 nm. The growth of the α' phase is restricted by the lamellar twin boundaries. Meanwhile, it can be seen that low density dislocation inside the α' phase and distinct boundary around the α' phase. This indicates that recovery has taken place during the severe plastic deformation. In detail, high density dislocation rearrangement and annihilation occur in the vicinity of dense dislocation walls and dislocation tangles in order to reduce the system energy. To make sure the phase constitution of the deformation microstructure, selected area electron diffraction (SAED) pattern in Fig. 1c is carried out. The SAED pattern indicates the composite diffractions of γ -matrix, α' -martensite and the deformation twins.

In order to analyze the effect of annealing on microstructure and mechanical properties, SMAT 30 min sample is annealed at 750 °C for 10 min under vacuum. What is interesting is that a band with about 2.5 μm width which is composed of plenty of new ultrafine subgrains is obtained in Fig. 2a. The band passes through the twin lamellar structure and is hindered by high density dislocation boundaries. The intersection angle between the band and the twin lamellar structure is about 71°. This phenomenon implies that recrystallization has taken place in the local region after annealing. However, the recrystallization phenomenon is not conspicuous near the band. Fig. 2b is an enlarged image of Fig. 2a which shows ultrafine subgrains with low dislocation density. In addition to equiaxed ultrafine subgrains, annealing twins (indicated by black arrows) are visible in Fig. 2c in the interior of the band.

Recovery and recrystallization can take place at high annealing temperature. As we know, the

dominant plastic deformation mode of 304L stainless steel is mechanical twinning at high strain or high strain rates prior to annealing [1,2], as indicated in Fig. 1. High density dislocation structures, such as dislocation cells and dense dislocation walls are visible in twin interiors and along the twin boundaries. After annealing at 750°C for 10 min, recrystallization is prone to take place in the region of high density dislocations because of the relative high stored deformation energies. It is difficult for deformation twinning to move at high temperature, so the slip of dislocations become the main deformation mode. The dislocations can easy move into high density twin boundaries, leading to a decrease in energies and more distinguishable boundaries.

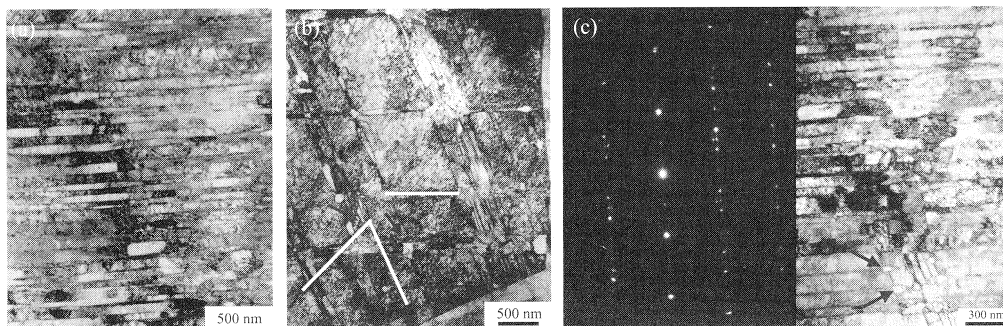


Fig.1 Cross-sectional TEM image of SMAT 304L SS. (a) lamellar structures at the depth of about 30 μm , (b) the intersection of deformation twins in three directions, (c) SAED patterns and the relative microstructure

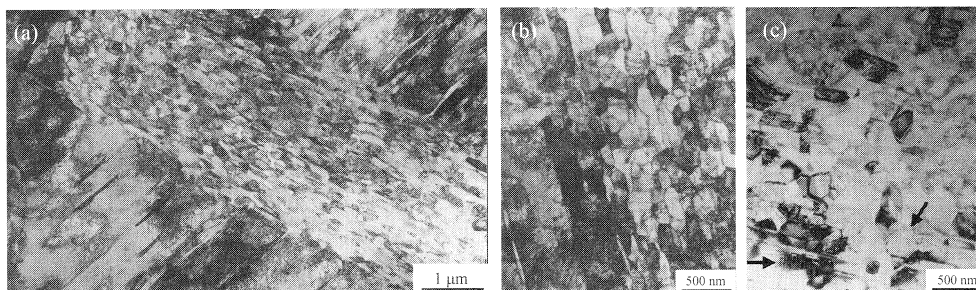


Fig. 2 The cross-sectional TEM image of SMAT 304L SS after annealing at the depth of about 30 μm deep, (a) a band with about 2.5 μm width composed of plenty of new ultrafine subgrains, (b) an enlarged region of (a), (c) ultrafine subgrains and annealing twins

Mechanical Properties. Effect of the SMAT process time and annealing temperature on the strength and the elongation is investigated. Fig. 3 shows the engineering stress-strain curves for the different SMAT time conditions and annealing temperature. For comparison, the curve of an annealed coarse-grained sample as the samples subjected to SMAT is also plotted. The yield strength ($\sigma_{0.2}$), the ultimate tensile strength (σ_{UTS}) and the uniform elongation (ϵ_u) are determined from the stress-strain curves and are listed in Table 1. The bulk samples with GNsL have several significant features compared to the coarse-grained sample. Firstly, the yield strength has been significantly increased for the SMAT samples, over the annealed sample. The yield strength has been increased by about 100% for the 15- and 30- processed samples. However, with SMAT process time increases, the potential for further improving yield strength declines. A slight increase in yield strength is obtained after the SMAT 15- and 30 min process. The ultimate tensile strength increases slightly with the increase of the process time. As we know, a great quantity of dislocations and deformation twins on the top surface are induced during the SMAT process. When the treatment is more severe, high density dislocation slip and interaction become more difficult, so that the increase in the yield strength becomes weak. Secondly, the uniform elongation decreases from about 64% for the annealed sample to 55% and 44% for the 2- and 15min processed samples, respectively. Thirdly, the elastic modulus has decreased after

SMAT process which is reported recently [15]. The yield strength and the ultimate tensile strength for the 650°C annealing sample are 485 and 761 MPa, respectively, slightly lower than that in the SMAT 30 min sample (yield strength of 570 MPa and ultimate tensile strength of 838 MPa). Compared with the SMAT 10min sample, the SMAT+annealed sample shows a litter higher yield strength and uniform elongation. Therefore a proper heat process is required to balance the strength and the elongation.

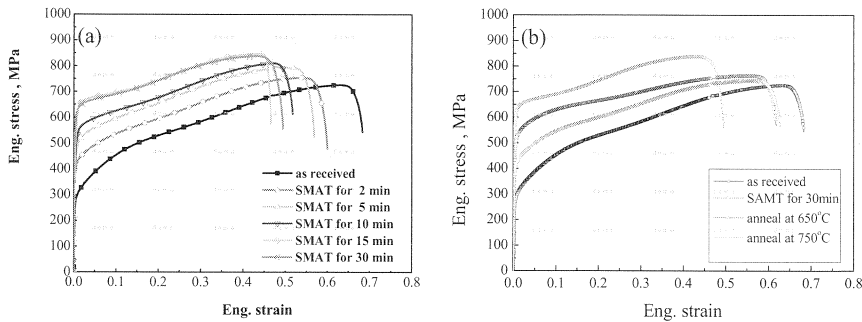


Fig. 3 Tensile stress-strain curves obtained for different SMAT process time (a) and different annealing temperature (b)

In addition, the strain hardening exponent (n) which is derived by fitting the Hollomon equation is calculated to evaluate strain hardening ability for all the experimental samples. The results are shown in Table 2. With increasing the SMAT process time, the n values follow a gradual decrease. The n value of the SMAT 30min sample is fitted to 0.076, much lower than that of the as-annealed sample ($n=0.241$). The decrease of the n values may result from the high density dislocation and low dislocation storage ability because of the tiny grains on the top surface.

Table 1 Mechanical properties of the as-received, deformed and annealed samples.

	E (GPa)	$\sigma_{0.2}$ (MPa)	σ_{UTS} (MPa)	ϵ_u (%)
As-received	156	275	726	64
SMAT 2 min	137	378	754	55
SMAT 5 min	129	422	800	51
SMAT 10 min	128	477	812	48
SMAT 15 min	128	552	846	44
SMAT 30 min	130	570	838	44
SMAT 30 min + 650 °C 10 min	162	485	761	58
SMAT 30 min + 750 °C 10 min	188	399	745	58

Table 2 Strain hardening exponent of as-received and the SMAT process samples

	As-received	SMAT 2 min	SMAT 5 min	SMAT 10 min	SMAT 15 min	SMAT 30 min
n	0.241	0.148	0.122	0.101	0.075	0.076

Summary

The microstructure characteristic and mechanical properties after SMAT process and subsequent annealing are investigated in a 304L SS. The prominent microstructural features involve the intersection of multi-system twin operation, subdividing the original grains into blocks, a martensite transformation mainly occurring at the interface of the twins as well, and the randomly orientated nanocrystallites on the top of surface. Recovery had occurred and the dislocation density was much reduced after annealing. The vast majority of the grains on the top surface are in the nanocrystalline/ultrafine range, with some recrystallization regions. The yield strength is about 2 times higher than that of the coarse-grained counterpart, but with a decrease in uniform elongation and elongation to failure as well.

Acknowledgments

The authors gratefully appreciate to the financial support by National Natural Science Foundation of China (NSFC) under Grant No. No. 10721202, and No. 010CB631000.

References

- [1] H.W. Zhang, Z.K. Hei, G. Liu, J. Lu and K. Lu: *Acta. Mater.* Vol. 51 (2003), p. 1871
- [2] C.X. Huang, G. Yang, Y.L. Gao, S.D. Wu and Z.F. Zhang: *Mater. Sci. Eng. A* Vol. 485 (2008), p. 643
- [3] J.Z. Lu, K.Y. Luo, Y.K. Zhang, G.F. Sun, Y.Y. Gua, J.Z. Zhou, X.D. Ren, X.C. Zhang, L.F. Zhang, K.M. Chen, C.Y. Cui, Y.F. Jiang, A.X. Feng and L. Zhang: *Acta Mater.* Vol. 58 (2010), p. 5354
- [4] K. Lu and J. Lu: *J. Mater. Sci. Technol.* Vol. 15(1999), p. 193
- [5] N.R. Tao, M.L. Sui, J. Lu and K. Lu: *Nanostruct. Mater.* Vol. 11(1999), p.433
- [6] K. Lu and J. Lu: *Mater. Sci. Eng. A* Vol. 375-377 (2004), p.38
- [7] N.R. Tao, Z.B. Wang, W.P. Tong, J. Lu and K. Lu: *Acta. Mater.* Vol. 50 (2002), p.4603
- [8] K. Wang, N.R. Tao, G. Liu, J. Lu and K. Lu: *Acta. Mater.* Vol. 54 (2006), p.5281
- [9] K.Y. Zhu, A. Vassel, F. Brisset, K. Lu and J. Lu: *Acta. Mater.* Vol. 52 (2004), p.4101
- [10] X.H. Chen, J. Lu, L. Lu and K. Lu: *Scripta Mater.* Vol. 52 (2005), p.1039
- [11] T. Roland, D. Reiraint, K. Lu and J. Lu: *Mater. Sci. Eng. A* Vol. 445-446 (2007), p.281
- [12] Y. M. Wang, K. Wang, D. Pan, K. Lu, K.J. Hemker and E. Ma: *Scripta Mater.* Vol. 48 (2003), p.1581
- [13] L.E. Murr, K.P. Staudhammer and S.S. Hecker: *Metall. Trans. A* Vol. 13 (1982), p.627
- [14] K.A. Johnson, L. E. Murr and K.P. Staudhammer: *Acta. Metall.* 37 (1985), p.677
- [15] J.W. Tian, K. Dai, J.C. Villegas, L. Shaw, P.K. Liaw, D.L. Klarstrom and A.L. Ortiz: *Mater. Sci. Eng. A* Vol. 493 (2008), p.176